

## Solution and Solid-State Structural Studies of Epoxide Adducts of Cadmium Phenoxides. Chemistry Relevant to Epoxide Activation for Ring-Opening Reactions

Donald J. Darensbourg,\* Jacob R. Wildeson, Samuel J. Lewis, and Jason C. Yarbrough

Contribution from the Department of Chemistry, Texas A&M University, College Station, Texas 77843

Received February 5, 2002

**Abstract:** The reaction of  $\text{Cd}[\text{N}(\text{SiMe}_3)_2]_2$  with 2 equiv of the corresponding phenol in toluene has led to the isolation of  $[\text{Cd}(\text{O}-2,6\text{-R}_2\text{C}_6\text{H}_3)_2]_2$  derivatives, where R represents the sterically bulky  $^t\text{Bu}$  and Ph substituents. The dimeric nature of these complexes in the solid state has been established via X-ray crystallography, i.e., trigonal geometry around cadmium is observed in **1** (R =  $^t\text{Bu}$ ) where the two cadmium centers are bridged by two phenoxides with each metal containing a terminal phenoxide. Complex **2** (R = Ph) contains an additional interaction of the metal centers with carbon atoms of the aromatic substituents on the phenoxide ligands. These dimeric structures are maintained in weakly coordinating solvents as revealed by  $^{113}\text{Cd}$  NMR in  $d_2$ -methylene chloride, which displays  $^{111}\text{Cd}$ – $^{113}\text{Cd}$  coupling. Nevertheless, because of the excessive steric requirements of these phenoxide ligands, these dimers are easily disrupted in solution by weak donor ligands such as epoxides. Three bisepoxide adducts have been isolated as crystalline solids and characterized by X-ray crystallography. As previously observed in other  $\text{Cd}(\text{O}-2,6\text{-}^t\text{Bu}_2\text{C}_6\text{H}_3)_2\cdot\text{L}_2$  complexes, these epoxide adducts adopt a crystallographically imposed square-planar geometry about the cadmium centers, with the exception of the *exo*-2,3-epoxynorbornane derivative, which displays a distorted tetrahedral geometry. Temperature-dependent  $^{113}\text{Cd}$  NMR studies have established that there is little difference in the binding abilities of these epoxides with either complex **1** or complex **2**. Importantly, it is concluded from these studies that the lack of reactivity of  $\alpha$ -pinene oxide and *exo*-2,3-epoxynorbornane toward copolymerization reactions with carbon dioxide, in the presence of zinc bisphenoxide catalysts, is not due to differences in epoxide metal binding. This is further affirmed by the isolation and crystallographic characterization of the very stable  $\text{Zn}(\text{O}-2,6\text{-}^t\text{Bu}_2\text{C}_6\text{H}_3)_2\cdot(\textit{exo}\text{-}2,3\text{-epoxynorbornane})_2$  derivative.

### Introduction

Presently, most of the commercially produced polycarbonates are formed from the polycondensation of phosgene and diols.<sup>1</sup> Notable exceptions are polypropylene carbonate and polyethylene carbonate which can also be synthesized from  $\text{CO}_2$  and the corresponding epoxide in the presence of rather ineffective heterogeneous zinc catalysts.<sup>2</sup> Hence, it is desirable to produce polycarbonates via this latter environmentally benign route utilizing more effective homogeneous catalysts. These efforts are intensified by the growing demand for these biodegradable thermoplastics for a variety of important applications.<sup>3</sup> In this regard there have been tremendous gains made recently in the area of homogeneously catalyzed production of polycarbonates from carbon dioxide and *alicyclic* epoxides, e.g., cyclohexene

oxide.<sup>4</sup> Nevertheless, these advances are somewhat overshadowed by the current lack of applications for these particular polymers.<sup>5</sup> On the other hand, these catalyst systems have been rather ineffective at coupling carbon dioxide and *aliphatic* epoxides to afford polycarbonates, instead yielding mostly cyclic carbonates.

We have recently been interested in finding alternative alicyclic epoxides that react with carbon dioxide to provide copolymers with  $T_g$  values more closely resembling that of the widely applicable bisphenol-A polycarbonate.<sup>6</sup> To this end we report herein comparative metal binding studies of Group 12

\* Corresponding author. E-mail: djdarens@mail.chem.tamu.edu.

- (1) *Engineering Thermoplastics: Polycarbonates, Polyacetals, Polyesters, Cellulose Esters*; Bottenbruch, L., Ed.; Hanser Publishing: New York, 1996; p 112.
- (2) PAC Polymers Inc., a subsidiary of Axess Corporation, 100 Interchange Boulevard, Newark, DE 19711.
- (3) Cowie, J. M. G. *Polymers: Chemistry and Physics of Modern Materials*, 2nd ed.; Blackie Academic and Professional: London, UK, 1991.

- (4) (a) Darensbourg, D. J.; Holtcamp, M. W. *Macromolecules* **1995**, *28*, 7577. (b) Super, M.; Berluche, E.; Costello, C.; Beckman, E. *Macromolecules* **1997**, *30*, 368. (c) Super, M.; Beckman, E. *J. Macromol. Symp.* **1998**, *127*, 89. (d) Cheng, M.; Lobkovsky, E. B.; Coates, G. W. *J. Am. Chem. Soc.* **1998**, *120*, 11018. (e) Darensbourg, D. J.; Holtcamp, M. W.; Struck, G. E.; Zimmer, M. S.; Niezgodna, S. A.; Rainey, P.; Robertson, J. B.; Draper, J. D.; Reibenspies, J. H. *J. Am. Chem. Soc.* **1999**, *121*, 107. (f) Darensbourg, D. J.; Wildeson, J. R.; Yarbrough, J. C.; Reibenspies, J. H. *J. Am. Chem. Soc.* **2000**, *122*, 12487. (g) Cheng, M.; Moore, D. R.; Reczek, J. J.; Chamberlain, B. M.; Lobkovsky, B. E.; Coates, G. W. *J. Am. Chem. Soc.* **2001**, *123*, 8738.
- (5) Beckman, E. *J. Science* **1999**, 283, 946.
- (6) Koning, C.; Wildeson, J.; Parton R.; Plum, B.; Steeman, P.; Darensbourg, D. J. *Polymer* **2001**, *42*, 3995.

metals with cyclohexene oxide, *exo*-2,3-epoxynorbornane, and  $\alpha$ -pinene oxide, as well as the relative activities of these epoxides to afford polycarbonates via the homogeneously catalyzed carbon dioxide coupling route. Specifically, we have investigated the binding of these alicyclic epoxides with cadmium phenoxides both in solution by  $^{113}\text{Cd}$  NMR and in the solid state by X-ray crystallography. In addition, the binding of *exo*-2,3-epoxynorbornane with  $[(2,6\text{-}^i\text{Bu}_2\text{C}_6\text{H}_3\text{O})_2\text{Zn}]_2$ , one of the known active catalysts for the coupling of cyclohexene oxide and carbon dioxide to produce polycarbonate,<sup>4a,e</sup> is examined by X-ray crystallography.

## Experimental Section

**Methods and Materials.** Unless otherwise specified, all syntheses and manipulations were carried out on a double manifold Schlenk vacuum line under an atmosphere of argon or in an argon-filled glovebox. Glassware was flamed dried thoroughly prior to use. Solvents were freshly distilled from sodium benzophenone before use. 2,6-Di-*tert*-butylphenol and 2,6-diphenylphenol were purchased from Aldrich Chemical Co. and were sublimed and stored in a glovebox. Both cyclohexene oxide and  $\alpha$ -pinene oxide were purified by distillation over calcium hydride. *exo*-2,3-epoxynorbornane was purchased from Aldrich Chemical Co. and stored in a glovebox prior to use.  $\text{Zn}[\text{N}(\text{SiMe}_3)_2]_2$  and  $\text{Cd}[\text{N}(\text{SiMe}_3)_2]_2$  were prepared according to the published literature,<sup>7</sup> stored in the glovebox, and used immediately after removal from the box. Infrared spectra were recorded on a Mattson 6081 spectrometer with DTGS and mercury cadmium telluride (MCT) detectors. All isotopically labeled solvents for NMR experiments were purchased from Cambridge Isotope Laboratories.  $^1\text{H}$  and  $^{13}\text{C}$  NMR spectra were recorded on Varian XL-200E, Unity +300 MHz, and VXR 300 MHz superconducting high-resolution spectrometers. Solution-state  $^{113}\text{Cd}$  spectra were recorded on a Varian XL-400 superconducting high-resolution spectrometer operating at 88 MHz using an external 0.1 M  $\text{Cd}(\text{ClO}_4)_2/\text{D}_2\text{O}$  reference. Crystals suitable for X-ray analysis of complexes **1**–**5** and **7** were obtained, and X-ray data were collected at 110 K on a Bruker Smart 1000 CCD diffractometer.<sup>8–12</sup> Elemental analyses were carried out by Galbraith Laboratories Inc.

*Note! Cadmium compounds and their wastes are extremely toxic and must be handled carefully. Cadmium waste products should be stored in a separate, clearly marked container.*

**Synthesis of  $[\text{Cd}(\text{O}-2,6\text{-}^i\text{Bu}_2\text{C}_6\text{H}_3)_2]_2$  (**1**).** A 5-mL toluene solution (0.190 g, 0.92 mmol) of 2,6-di-*tert*-butyl phenol was added to a 5-mL toluene solution of  $\text{Cd}[\text{N}(\text{SiMe}_3)_2]_2$  (0.20 g, 0.46 mmol). After being stirred for 1 h at ambient temperature the clear light yellow/orange solution was vacuum-dried and the resulting yellow solid was recrystallized from a minimum amount of methylene chloride at  $-20^\circ\text{C}$ . The supernate was transferred using a cannula and the crystals dried under vacuum to yield 0.175 g of product (72.5%). Anal. Calcd for  $\text{C}_{56}\text{H}_{84}\text{O}_4\text{-Cd}_2$ : C, 64.28; H, 8.11. Found: C, 63.37; H, 8.31.  $^1\text{H}$  NMR ( $\text{CD}_2\text{Cl}_2$ ) for bridging and terminal ligands respectively:  $\delta$  1.13, 1.59 [s, 18H,  $\{-\text{CMe}_3\}$ ]; 6.46, 6.82 [t, 1H,  $\{4\text{-H}\}$ ]; 6.92, 7.21 [d, 2H,  $\{3,5\text{-H}\}$ ].  $^{13}\text{C}\{^1\text{H}\}$  NMR( $\text{CD}_2\text{Cl}_2$ ):  $\delta$  31.1, 33.6  $\{-\text{CMe}_3\}$ ; 35.6, 36.5  $\{-\text{CMe}_3\}$ ; 116.7, 121.2  $\{4\text{-C}_6\text{H}_3\}$ ; 125.0, 127.4  $\{3, 5\text{-C}_6\text{H}_3\}$ ; 136.5, 139.9  $\{2,6\text{-C}_6\text{H}_3\}$ ; 165.5  $\{ipso\text{-C}_6\text{H}_3\}$ .  $^{113}\text{Cd}\{^1\text{H}\}$  NMR ( $\text{CD}_2\text{Cl}_2$ ):  $\delta$  7.17 ( $J^{113}\text{Cd}\text{-}^{111}\text{Cd} = 117$  Hz).

**Synthesis of  $[\text{Cd}(\text{O}-2,6\text{-Ph}_2\text{C}_6\text{H}_3)_2]_2$  (**2**).** A 5-mL toluene solution (0.228 g, 0.92 mmol) of 2,6-diphenyl phenol was added to a 5-mL toluene solution of  $\text{Cd}[\text{N}(\text{SiMe}_3)_2]_2$  (0.200 g, 0.46 mmol), and the clear pale yellow solution was allowed to stir for 1 h at ambient temperature. The solution was dried under vacuum and the light yellow solid was recrystallized from a minimum amount of methylene chloride at  $-20^\circ\text{C}$ . The supernate was removed using a cannula and the crystals were dried under vacuum to yield 0.191 g of product (68.6%). Anal. Calcd for  $\text{C}_{72}\text{H}_{52}\text{O}_4\text{Cd}_2$ : C, 71.69; H, 4.35. Found: C, 69.66; H, 4.61.  $^1\text{H}$  NMR ( $\text{CD}_2\text{Cl}_2$ ) for bridging and terminal ligands respectively at  $-40^\circ\text{C}$ :  $\delta$  6.87–7.79 [br, 13H,  $\{2, 6\text{-Ph}_2\text{C}_6\text{H}_3\}$ ].  $^{13}\text{C}\{^1\text{H}\}$  NMR ( $\text{CD}_2\text{Cl}_2$ ):  $\delta$  125.9–131.6  $\{\text{Ph}_2\text{C}_6\text{H}_3\}\{3,4,5\text{-C}_6\text{H}_3\}$ ; 140.4, 140.7  $\{2,6\text{-C}_6\text{H}_3\}$ ; 155.1, 160.4  $\{ipso\text{-C}_6\text{H}_3\}$ .  $^{113}\text{Cd}\{^1\text{H}\}$  NMR ( $\text{CD}_2\text{Cl}_2$ ):  $\delta$  77.43 ( $J^{113}\text{Cd}\text{-}^{111}\text{Cd} = 95$  Hz).

### High-Pressure Copolymerization of $\text{CO}_2$ with $\alpha$ -Pinene Oxide.

A sample of the catalyst  $[\text{Zn}(\text{O}-2,6\text{-F}_2\text{C}_6\text{H}_3)_2\text{THF}]_2$  (0.100 g) was dissolved in 20.0 mL of  $\alpha$ -pinene oxide. The solution was loaded via a syringe port into a 150 mL stainless steel Parr autoclave that had previously been dried overnight under vacuum at  $80^\circ\text{C}$ . Two sets of experiments were performed. The first involved a reaction pressurized to 42 bar with  $\text{CO}_2$  and then heated to  $80^\circ\text{C}$  for a 24–48 h reaction period. The second varied from the first by raising the reaction temperature from  $80^\circ\text{C}$  to  $120^\circ\text{C}$ . In addition,  $\alpha$ -pinene oxide was also tested for its ability to terpolymerize with  $\text{CO}_2$  and cyclohexene oxide by using a mixture of monomers (70 mol % cyclohexene oxide and 30 mol %  $\alpha$ -pinene oxide). After allowing the reactor to cool to ambient temperature, the reaction mixture was diluted with  $\text{CH}_2\text{Cl}_2$  and analyzed by infrared spectroscopy in the  $\nu(\text{CO}_2)$  region.

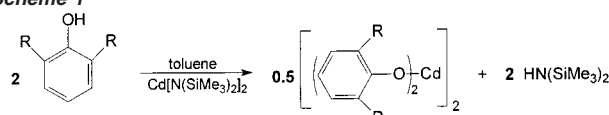
### High-Pressure Copolymerization of $\text{CO}_2$ with *exo*-2,3-Epoxynorbornane.

A sample of the catalyst  $[\text{Zn}(\text{O}-2,6\text{-F}_2\text{C}_6\text{H}_3)_2\text{THF}]_2$  (0.100 g) was dissolved in 16.0 mL of a toluene/epoxynorbornane solution, which was prepared by dissolving 10.00 g of epoxynorbornane in 12.0 mL of toluene. The resulting solution was loaded via a syringe port into a 150 mL stainless steel Parr autoclave that had previously been dried overnight under vacuum at  $80^\circ\text{C}$ . Similar to the experiments performed with  $\alpha$ -pinene oxide monomer, two sets of reactions were performed. The first involved a reaction pressurized to 42 bar with  $\text{CO}_2$  and heated to  $80^\circ\text{C}$  for a 24–48 h reaction period. The second varied from the first by raising the reaction temperature from  $80^\circ\text{C}$  to  $120^\circ\text{C}$ . As with the  $\alpha$ -pinene oxide, epoxynorbornane was also tested for its ability to terpolymerize with  $\text{CO}_2$  and cyclohexene oxide by using a mixture of monomers (70 mol % cyclohexene oxide and 30 mol % epoxynorbornane). Analysis of the reaction mixture was carried out as described above using infrared spectroscopy in the  $\nu(\text{CO}_2)$  region.

## Results and Discussion

The dimeric cadmium phenoxide derivatives were synthesized by the pathway described below and isolated in purified yields of greater than 68%. That is,  $\text{Cd}[\text{N}(\text{SiMe}_3)_2]_2$  was reacted with 2 equiv of the corresponding phenol in a toluene medium (Scheme 1). The resulting light yellow solutions were allowed to stir at ambient temperature for 2 h, and the product was isolated by vacuum removal of the solvent. Crystals suitable for X-ray crystallography were obtained by dissolving the solid product in a minimum quantity of methylene chloride and cooling the solution at  $-20^\circ\text{C}$  for 3–4 days.

### Scheme 1



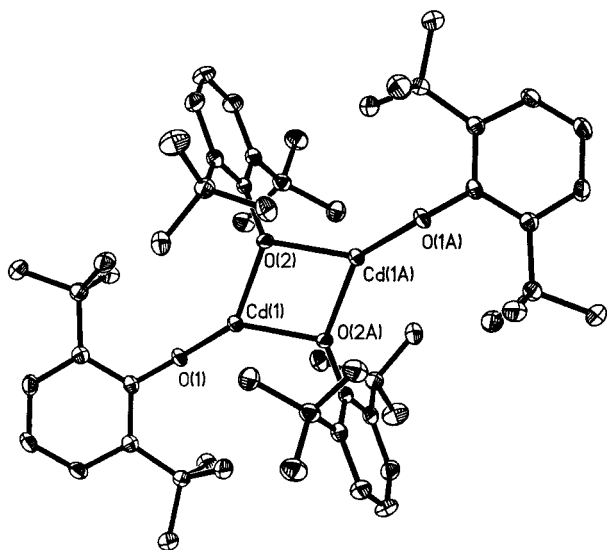
	R
1	<i>tert</i> -butyl
2	phenyl

- (7) Burger, H.; Sawodny, W.; Wannagat, V. *J. Organomet. Chem.* **1965**, *3*, 113.  
 (8) SMART 1000 CCD; Bruker Analytical X-ray Systems: Madison, WI, 1999.  
 (9) Bruker, SAINT-Plus, version 6.02; Madison, WI, 1999.  
 (10) Sheldrick, G. SHELXS-86, Program for Crystal Structure Solution; Institut für Anorganische Chemie der Universität: Tammanstrasse 4, D-3400 Göttingen, Germany, 1986.  
 (11) Sheldrick, G. SHELXL-97, Program for Crystal Structure Refinement; Institut für Anorganische Chemie der Universität: Tammanstrasse 4, D-3400 Göttingen, Germany, 1997.  
 (12) Bruker, SHELXTL, version 5.0; Madison, WI, 1999.

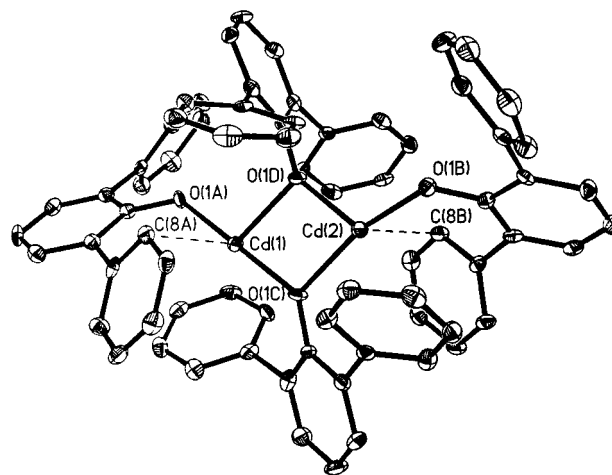
**Table 1.** Selected Bond Distances (Å) and Bond Angles (deg) for Complexes **1** and **2**<sup>a</sup>

Complex 1			
Cd(1)–O(1)	2.0422(15)	Cd(1)–O(2)	2.1773(17)
Cd(1)–O(2A)	2.1954(17)	O(1)–C(1)	1.356(2)
O(2)–C(15)	1.374(2)		
O(1)–Cd(1)–O(2)	142.01(6)	O(1)–Cd(1)–O(2A)	136.30(6)
O(2)–Cd(1)–O(2A)	76.67(6)	Cd(1)–O(2)–Cd(1A)	103.33(6)
Cd(1)–O(2)–C(15)	133.50(12)	Cd(1)–O(1)–C(1)	136.05(12)
Complex 2			
Cd(1)–O(1A)	2.063(3)	Cd(2)–O(1B)	2.080(3)
Cd(1)–O(1D)	2.231(3)	Cd(2)–O(1D)	2.202(3)
Cd(1)–O(1C)	2.158(3)	Cd(2)–O(1C)	2.186(3)
Cd(1)–C(8A)	2.680(5)	Cd(2)–C(8B)	2.622(5)
O(1A)–C(1A)	1.325(5)	O(1B)–C(1B)	1.331(6)
O(1C)–C(1C)	1.357(5)	O(1D)–C(1D)	1.351(5)
O(1C)–Cd(1)–O(1D)	77.03(11)	O(1B)–Cd(2)–O(1D)	119.69(12)
O(1C)–Cd(2)–O(1D)	77.06(11)	O(1B)–Cd(2)–C(8B)	82.70(13)
Cd(1)–O(1C)–Cd(2)	104.35(12)	C(8B)–Cd(2)–O(1C)	102.16(13)
Cd(1)–O(1D)–Cd(2)	101.42(12)	C(8B)–Cd(2)–O(1D)	98.14(13)
O(1A)–Cd(1)–O(1D)	103.32(11)	Cd(2)–O(1B)–C(1B)	127.3(3)
O(1A)–Cd(1)–O(1C)	178.62(13)	Cd(2)–O(1D)–C(1D)	141.2(3)
C(8A)–Cd(1)–O(1A)	78.61(13)	Cd(2)–O(1C)–C(1C)	125.2(3)
C(8A)–Cd(1)–O(1C)	102.64(13)	Cd(1)–O(1A)–C(1A)	127.6(3)
C(8A)–Cd(1)–O(1D)	102.34(13)	Cd(1)–O(1D)–C(1D)	116.1(3)
O(1B)–Cd(2)–O(1C)	162.07(11)	Cd(1)–O(1C)–C(1C)	127.9(3)

<sup>a</sup> Estimated standard deviations are given in parentheses.

**Figure 1.** Thermal ellipsoid representation of complex **1**, [Cd(O-2,6-*t*-Bu<sub>2</sub>C<sub>6</sub>H<sub>3</sub>)<sub>2</sub>]<sub>2</sub>.

Complexes **1** and **2** have been characterized in the solid state by X-ray crystallography, and a list of selected bond lengths and angles is provided in Table 1. Figure 1 displays a thermal ellipsoid rendering of **1**, along with a partial atom-labeling scheme. The structure of complex **1** consists of a planar arrangement of the two cadmium atoms and the two oxygen atoms of the bridging phenoxide ligands which form a parallelogram with an O(2)–Cd(1)–O(2A) bond angle of 76.67(6)° and a Cd(1)–O(2)–Cd(1A) bond angle of 103.33(6)°. The cadmium centers in **1**, located 3.4298(13) Å from one another, are coordinated in a distorted trigonal planar geometry as seen in its zinc analogue,<sup>13</sup> with two bridging Cd–O bond distances (Cd(1)–O(2) and Cd(1)–O(2A)) of 2.1773(17) and 2.1954(17) Å, respectively. The terminal Cd(1)–O(1) bond distance at

**Figure 2.** Thermal ellipsoid representation of complex **2**, [Cd(O-2,6-Ph<sub>2</sub>C<sub>6</sub>H<sub>3</sub>)<sub>2</sub>]<sub>2</sub>.

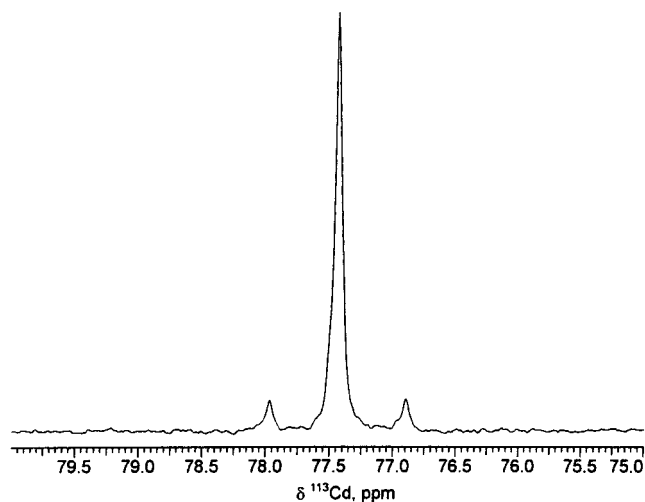
2.0422(15) Å is about 0.14 Å shorter than the bridging Cd–O distances. The remaining bond angles about the cadmium centers O(1)–Cd(1)–O(2) and O(1)–Cd(1)–O(2A) were found to be 142.01(6)° and 136.30(6)°.

Figure 2 shows a thermal ellipsoid representation of complex **2**, along with a partial atom-labeling scheme. By way of contrast, **2**, although dimeric, contains four-coordinate cadmium centers separated by 3.4314(8) Å which are each bonded to two bridging phenoxide, a terminal phenoxide, and an aromatic carbon atom from one of the phenyl substituents of the terminal phenoxide ligands. The parallelogram formed by the two cadmium atoms and bridging phenoxide oxygen atoms possesses average Cd–O–Cd and O–Cd–O bond angles of 102.9° and 77.0°, respectively. The average Cd–O bridging bond distance is 2.194[3] Å, whereas the average Cd–O terminal bond distance is 2.072[3] Å. The six-membered ring formed via interaction of cadmium with the terminal phenoxide ligand and one of the carbon atoms of its phenyl substituents is in a distorted chair conformation. The Cd(1)–C(8A) and Cd(2)–C(8B) bond distances at 2.680(5) and 2.622(5) Å, respectively, are slightly longer than the sum of the covalent radii of cadmium and carbon (2.25 Å) but considerably shorter than the sum of their van der Waal radii (3.28 Å). As a consequence of the interaction of cadmium with the aromatic carbon the angle formed by the bridging phenoxide–cadmium–terminal phenoxide, O(1C)–Cd(1)–O(1A), is nearly linear at 178.62(14)°. A similar less dramatic effect is seen at the Cd(2) center, where the O(1B)–Cd(2)–O(1C) angle was found to be 162.07(11)°. This additional interaction of the cadmium centers in **2** with the terminal phenoxide ligands by way of its phenyl substituents may account for the added stability of the dimer noted in solution (*vide infra*).

Complexes **1** and **2** remain dimeric upon dissolution in *d*<sub>2</sub>-methylene chloride as is evident from their <sup>113</sup>Cd or <sup>111</sup>Cd NMR spectra. Figure 3 displays the <sup>113</sup>Cd NMR spectrum of complex **2** at ambient temperature, where coupling is readily seen between the two cadmium spin states of *I* = 1/2 (i.e., <sup>111</sup>Cd (12.75%) and <sup>113</sup>Cd (12.26%)) with δ<sup>113</sup>Cd = 77.4 ppm and *J*<sup>113</sup>Cd–<sup>111</sup>Cd = 95 Hz. As expected from our previous studies, the <sup>113</sup>Cd NMR resonances are very dependent on the substituents on the phenoxide ligands.<sup>14</sup> In this instance, δ<sup>113</sup>Cd for

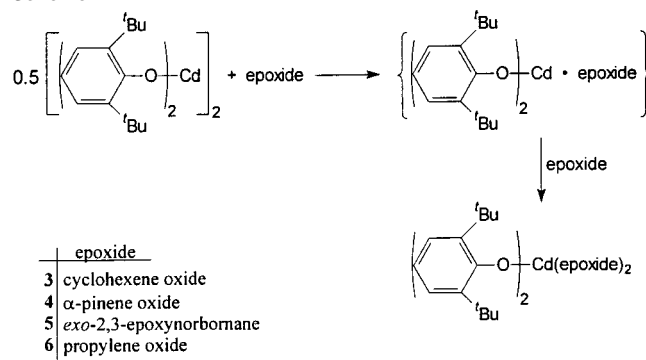
(13) Kunert, M.; Bräuer, M.; Klobes, O.; Görls, H.; Dinjus, E.; Anders, E. *Eur. J. Inorg. Chem.* **2000**, 1803.

(14) Darensbourg, D. J.; Niezgod, S. A.; Draper, J. D.; Reibenspies, J. H. *J. Am. Chem. Soc.* **1998**, *120*, 4690.



**Figure 3.**  $^{113}\text{Cd}$  NMR spectrum of  $[\text{Cd}(\text{O}-2,6\text{-Ph}_2\text{C}_6\text{H}_3)_2]$  in  $d_2$ -methylene chloride at ambient temperature.

#### Scheme 2



complex **1** is shifted significantly upfield at 7.17 ppm with a larger  $J^{113}\text{Cd}-^{111}\text{Cd}$  value of 117 Hz. Upon adding various epoxides to methylene chloride solutions of complex **1**, dimer disruption occurs with sequential formation of mononuclear mono- and bisepoxide adducts (Scheme 2). Several of the latter derivatives (**3–5**) have been isolated as single crystals and characterized by X-ray crystallography.

The cyclohexene oxide and  $\alpha$ -pinene oxide bisadducts, complexes **3** and **4**, both adopt a crystallographically imposed square-planar geometry about the metal center. This is akin to what is observed in the THF, THT(tetrahydrothiophene), and PC(propylene carbonate) analogues.<sup>14</sup> On the other hand, the bis-*exo*-2,3-epoxynorbornane adduct, complex **5**, exhibits a highly distorted tetrahedral arrangement of oxygen donor ligands about the cadmium center. Thermal ellipsoid representations of these cadmium derivatives, which are among the few structurally characterized metal epoxide complexes, are displayed in Figures 4–6.<sup>15–20</sup> Table 2 contains selected bond distances and bond angles for these epoxide complexes. Comparative bond distances in other published  $\text{Cd}(\text{O}-2,6\text{-}^i\text{Bu}_2\text{C}_6\text{H}_3)_2$  adducts are provided

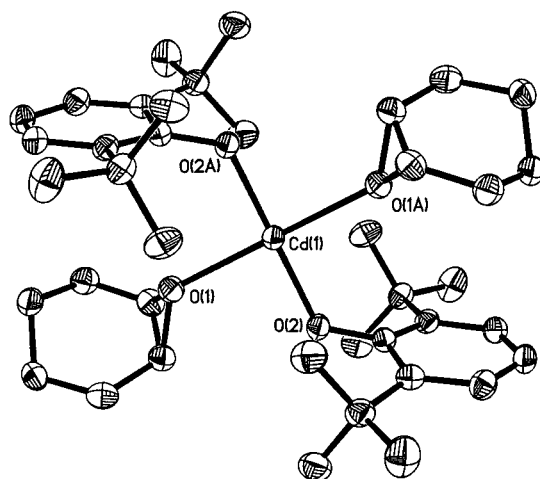


**Figure 4.** Thermal ellipsoid representation of complex **3**,  $[\text{Cd}(\text{O}-2,6\text{-}t\text{-Bu}_2\text{C}_6\text{H}_3)_2](\text{cyclohexene oxide})_2$ .

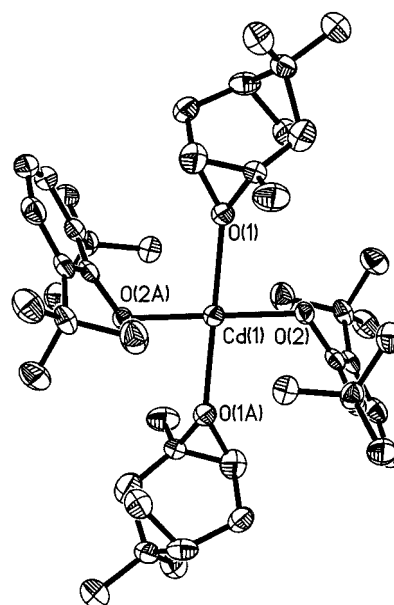


**Figure 5.** Thermal ellipsoid representation of complex **4**,  $[\text{Cd}(\text{O}-2,6\text{-}t\text{-Bu}_2\text{C}_6\text{H}_3)_2](\alpha\text{-pinene oxide})_2$ .

in Table 3. The Cd–O(epoxide) bond distances in complexes **3–5** span a very narrow range, 2.357(2) Å and 2.307[5] Å in the cyclohexene oxide and *exo*-2,3-epoxynorbornane derivatives, respectively. Unexpectedly, the Cd–O bond distance of the THF analog was found to be significantly longer at 2.465(3) Å.<sup>14,21</sup> The only notable difference in the solid-state structures of complexes **3** and **4** is the average of the two *carbon–O–cadmium* angles defining the epoxide cadmium interaction. Alternatively, this angle may be defined by the Cd–O vector and the midpoint of the OC<sub>2</sub> plane. In complex **3** this angle is found to be 127.52°, whereas in **4** it is more obtuse at 142.1°, i.e., it is more pyramidal in **3**. On the other hand, complex **5**, which has two crystallographically independently located epoxide ligands, displays analogous angles of 129.4° and 138.3°. The corresponding Cd–O(epoxide) bond distances in structurally characterized six-coordinate cyclic ether adducts of  $[\text{Tp}^{\text{Ph}}]\text{Cd}(\text{acetate})$ , where  $\text{Tp}^{\text{Ph}} = \text{hydrotris}(3\text{-phenylpyrazol-1-yl})$ -

(15) Groves, J. T.; Han, Y.; van Engen, D. *J. Chem. Soc., Chem. Commun.* **1990**, 436.

(16) Harder, S.; Boersma, J.; Brandsma, L.; Kanters, J. A.; Duisenberg, A. J. M.; van Lenthe, J. H. *Organometallics* **1990**, *9*, 511.

(17) Darensbourg, D. J.; Holtcamp, M. W.; Khandelwal, B.; Klausmeyer, K. K.; Reibenspies, J. H. *J. Am. Chem. Soc.* **1995**, *117*, 538.

(18) Darensbourg, D. J.; Niezgodna, S. A.; Holtcamp, M. W.; Draper, J. D.; Reibenspies, J. H. *Inorg. Chem.* **1997**, *36*, 2424.

(19) Dias, H. V. R.; Wang, Z. Y. *Inorg. Chem.* **2000**, *39*, 3724.

(20) Beckwith, J. D.; Tschinkl, M.; Picot, A.; Tsunoda, M.; Bachman, R.; Gabbai, F. P. *Organometallics* **2001**, *20*, 3169.

(21) Goel, S. C.; Chiang, M. Y.; Buhro, W. E. *J. Am. Chem. Soc.* **1990**, *112*, 6724.

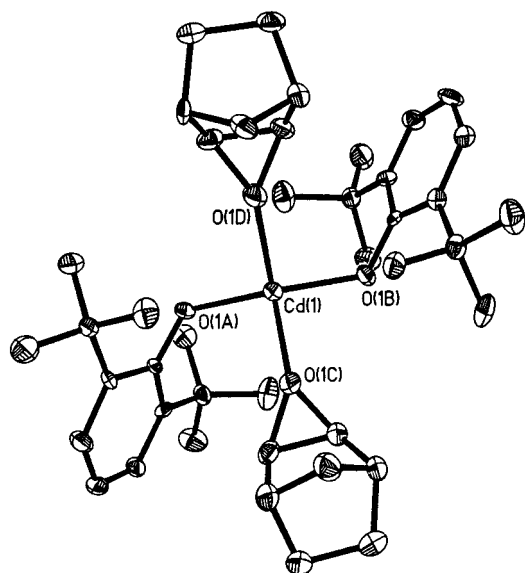


**Figure 6.** Thermal ellipsoid representation of complex **5**, [Cd(O-2,6-*t*-Bu<sub>2</sub>C<sub>6</sub>H<sub>3</sub>)<sub>2</sub>](*exo*-2,3-epoxynorbornane)<sub>2</sub>.

**Table 2.** Selected Bond Distances (Å) and Bond Angles (deg) for Complexes **3–5**<sup>a</sup>

Complex 3			
Cd(1)–O(1)	2.357(2)	Cd(1)–O(2)	2.0858(19)
O(1)–C(1A)	1.460(4)	O(1)–C(2A)	1.459(4)
O(2)–C(1B)	1.347(3)		
O(1)–Cd(1)–O(2)	86.50(8)	O(2)–Cd(1)–O(1A)	93.50(8)
C(2A)–O(1)–Cd(1)	128.15(17)	C(1A)–O(1)–Cd(1)	126.89(18)
C(1B)–O(2)–Cd(1)	122.56(17)		
Complex 4			
Cd(1)–O(1)	2.336(4)	Cd(1)–O(2)	2.063(4)
O(1)–C(1A)	1.485(9)	O(1)–C(2A)	1.455(8)
O(2)–C(1B)	1.349(7)		
O(1)–Cd(1)–O(2)	96.43(15)	O(2)–Cd(1)–O(1A)	83.57(15)
C(2A)–O(1)–Cd(1)	138.5(4)	C(1A)–O(1)–Cd(1)	145.6(4)
C(1B)–O(2)–Cd(1)	121.2(3)		
Complex 5			
Cd(1)–O(1A)	2.060(5)	Cd(1)–O(1B)	2.065(5)
Cd(1)–O(1C)	2.301(5)	Cd(1)–O(1D)	2.313(5)
O(1A)–C(1A)	1.345(7)	O(1B)–C(1B)	1.347(7)
O(1C)–C(1C)	1.471(8)	O(1C)–C(2C)	1.472(9)
O(1D)–C(2D)	1.464(9)	O(1D)–C(1D)	1.464(8)
O(1A)–Cd(1)–O(1B)	147.6(2)	O(1A)–Cd(1)–O(1D)	101.2(2)
O(1A)–Cd(1)–O(1C)	100.57(18)	O(1B)–Cd(1)–O(1D)	97.25(19)
O(1B)–Cd(1)–O(1C)	95.56(19)	O(1C)–Cd(1)–O(1D)	114.37(19)
C(1A)–O(1A)–Cd(1)	124.5(4)	C(1B)–O(1B)–Cd(1)	124.9(4)
C(1C)–O(1C)–Cd(1)	133.9(4)	C(2C)–O(1C)–Cd(1)	124.9(4)
C(2D)–O(1D)–Cd(1)	139.7(5)	C(1D)–O(1D)–Cd(1)	136.8(5)

<sup>a</sup> Estimated standard deviations are given in parentheses.

borate, similarly exhibit little variance,<sup>17,18</sup> nevertheless, the bond distance of the THF adduct is quite similar to the others. That is, these Cd–O bond distances increase along the following series: THF (2.388(8) Å) < cyclohexene oxide (2.395(4) Å) < propylene oxide (2.414(4) Å) < dioxane (2.448(7) Å).<sup>18</sup> Consistent with the similarities in Cd–O bond distances for the cyclic ether adducts in this latter series, the  $\Delta H^\circ$  parameters for binding, as determined by temperature-dependent <sup>113</sup>Cd NMR spectroscopy, did not vary notably.

Herein, we have in like fashion measured the epoxide interactions with the cadmium dimer complex, [Cd(O-2,6-*t*-Bu<sub>2</sub>C<sub>6</sub>H<sub>3</sub>)<sub>2</sub>]<sub>2</sub> (**1**), in the weakly interacting methylene chloride solvent (Scheme 2). Our ability to isolate single crystals of

**Table 3.** Comparative Bond Distances in Square-Planar Cd(O-2,6-*t*-Bu<sub>2</sub>C<sub>6</sub>H<sub>3</sub>)<sub>2</sub>L<sub>2</sub> Derivatives<sup>a</sup>

L	Cd–L (Å)	Cd–O (Å)	ref
tetrahydrofuran	2.498(5)	2.058(4)	16 <sup>b</sup>
	2.465(3)	2.068(3)	9 <sup>c</sup>
tetrahydrothiophene	2.768(2)	2.102(6)	9
propylene carbonate	2.393(8)	2.038(8)	9
cyclohexene oxide	2.357(2)	2.0858(19)	this work
$\alpha$ -pinene oxide	2.336(4)	2.063(4)	this work
<i>exo</i> -2,3-epoxynorbornane <sup>d</sup>	av 2.307[5]	2.063[5]	this work

<sup>a</sup> All complexes have crystallographically imposed square-planar geometry about Cd(II) except the last entry. <sup>b</sup> Determined at ambient temperature. <sup>c</sup> Determined at 193 K. <sup>d</sup> Complex has a distorted tetrahedral geometry about the Cd(II) center.

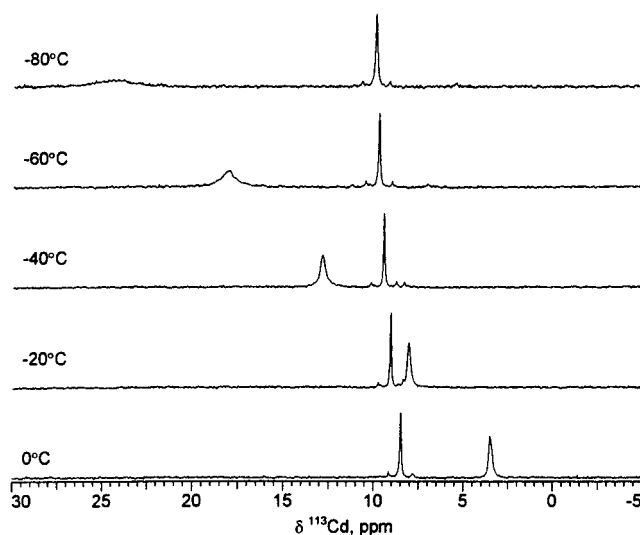


**Figure 7.** Temperature-dependent <sup>113</sup>Cd NMR spectra of complex **1** in the presence of 2 equiv of cyclohexene oxide in *d*<sub>2</sub>-methylene chloride.

complex **3–5** and demonstrate a close similarity in Cd–O(epoxide) bond distances strongly suggests that there is nothing particularly unique about cyclohexene oxide as compared to  $\alpha$ -pinene oxide and *exo*-2,3-epoxynorbornane with regard to metal binding and thereby activation.

Notwithstanding, it is of importance to establish the relative metal binding abilities of these particular epoxides since their reactivity toward homopolymerization to provide polyethers or copolymerization with CO<sub>2</sub> to afford polycarbonates are so divergent. That is cyclohexene oxide readily homopolymerizes or copolymerizes with CO<sub>2</sub> in the presence of catalysts such as Zn(O-2,6-*R*<sub>2</sub>C<sub>6</sub>H<sub>3</sub>)<sub>2</sub>·(THF)<sub>2</sub><sup>4a,e</sup> or [Zn(O-2,6-*F*<sub>2</sub>C<sub>6</sub>H<sub>3</sub>)<sub>2</sub>·THF]<sub>2</sub>,<sup>4f</sup> whereas  $\alpha$ -pinene and *exo*-2,3-epoxynorbornane exhibit *no* reactivity under similar conditions (*vide infra*).

Figures 7 and 8 contain several of the temperature-dependent <sup>113</sup>Cd NMR traces for the addition of 2 and 4 equiv of cyclohexene oxide(CHO) to the dimeric complex **1** in *d*<sub>2</sub>-methylene chloride. As is evident from the spectra in Figure 7, where 2 equiv of CHO were employed, initially there is a slight excess (about 10% more) of cadmium in the form of the monomer **1**·(CHO), (**3**<sup>−</sup>), relative to **1** + CHO at ambient temperature. That is the <sup>113</sup>Cd resonance at 7.17 ppm with  $J^{113\text{Cd}-111\text{Cd}} = 117$  Hz is due to the dimer, complex **1**, whereas the signal at ca. −0.90 ppm is assigned to the mono-epoxide adduct of the monomer of **1**, complex **3**<sup>−</sup>. Upon lowering the temperature the <sup>113</sup>Cd resonance due to **3**<sup>−</sup> shifts downfield with binding to the second equivalent of CHO to afford complex **3**.

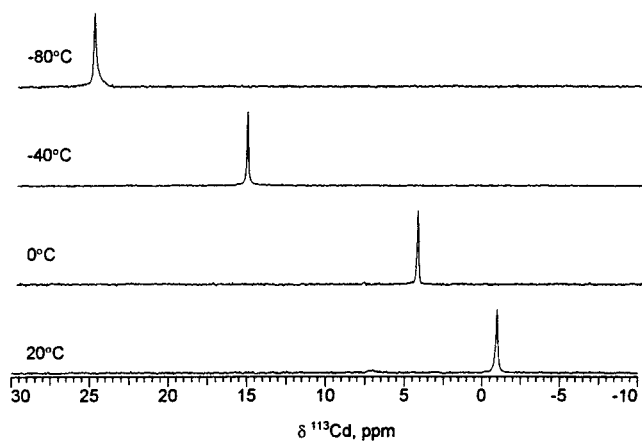


**Figure 8.** Temperature-dependent  $^{113}\text{Cd}$  NMR spectra of complex **1** in the presence of 4 equiv of cyclohexene oxide in  $d_2$ -methylene chloride.

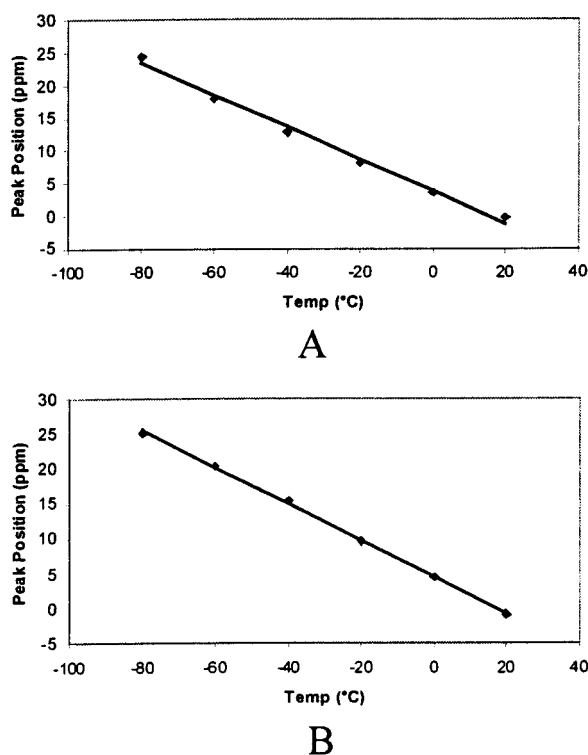


**Figure 9.** Plot of the  $^{113}\text{Cd}$  NMR signal for epoxide adducts of complex **1** as a function of temperature in the presence of (A) 2 equiv of cyclohexene oxide and (B) 4 equiv of cyclohexene oxide.

Proton NMR monitoring of the epoxide when bound and free is consistent with this interpretation. The addition of 4 equiv of CHO to **1** at ambient temperature initially results in >90% of cadmium existing in the form of complex **3**<sup>-</sup>; again upon lowering the temperature the  $^{113}\text{Cd}$  resonance derived from a rapid exchange of epoxide ligand between complex **3** and **3**<sup>-</sup> exhibits a linear dependence on temperature (see Figure 9), ultimately ending up at approximately 25 ppm at  $-80^\circ\text{C}$ . This latter signal is assigned to complex **3**. Similar observations were noted when complex **1** is reacted with 200 equiv of CHO. As seen in Figure 7, there is a small downfield shift ( $\sim 2$  ppm) of the  $^{113}\text{Cd}$  resonance for complex **1** as the temperature is lowered from ambient to  $-60/-80^\circ\text{C}$ . Also noted in Figure 7, where the [epoxide] is deficient (mol Cd monomer/mol epoxide = 0.54), ligand exchange between **3** and **3**<sup>-</sup> is slowed as the temperature is lowered, where at  $-80^\circ\text{C}$  there is significant

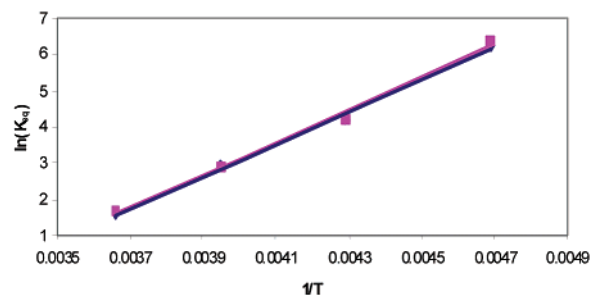
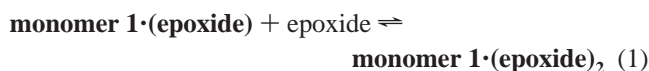


**Figure 10.** Plots of the  $\ln K_{\text{eq}}$  vs  $1/T$  for the equilibrium process defined in eq 1 for the two sets of conditions described in Figure 9: A ( $\blacktriangle$ ) and B ( $\blacksquare$ ).

line broadening of the signal due to the predominant species in solution, complex **3**. Because of solvent limitations, it was not possible to reduce the temperature further and reach the very slow exchange limit.

From data such as those provided in Figure 9, coupled with the initial concentrations of the dimeric cadmium complex (**1**) and cyclohexene oxide, it is possible to calculate the equilibrium constant between complex **3**<sup>-</sup> plus cyclohexene oxide and complex **3** (eq 1) as a function of temperature.<sup>22</sup> That is, it can



be assumed that the average  $^{113}\text{Cd}$  chemical shift position is directly proportional to the percentage of each monomeric cadmium species present in solution. Hence, temperature-dependent  $K_{\text{eq}}$  values for the process defined in eq 1 were computed for two different sets of initial epoxide concentrations. Representative plots of  $\ln K_{\text{eq}}$  vs  $T^{-1}$  for two different experiments involving the binding of cyclohexene oxide to the monomer of complex **1** are given in Figure 10. Calculation of the enthalpy, entropy, and free energy of the equilibrium defined in eq 1 are summarized in Table 4, where the epoxide is varied from cyclohexene oxide to *exo*-2,3-epoxynorbornane.

As is obvious from the data listed in Table 4 the binding abilities of cyclohexene oxide and *exo*-2,3-epoxynorbornane do not differ significantly. Indeed, this observation is consistent with the similarity in the Cd–O<sub>epoxide</sub> bonding distances found in the solid-state structures of complexes **3** and **5**, despite the difference in the geometries of these two derivatives. Qualitatively, the binding of the epoxides,  $\alpha$ -pinene oxide and propylene oxide, to the monomer of complex **1** is similar to that quantitatively assessed above. Assuming the *relative* binding ability of these epoxides to the metal center of Cd(O-2,6-<sup>t</sup>Bu<sub>2</sub>C<sub>6</sub>H<sub>3</sub>)<sub>2</sub> is not considerably different from that in the zinc analogues, this observation is in stark contrast to the relative ease of copolymerization of these epoxides with CO<sub>2</sub> to afford polycarbonates (vide infra).

Finally, it was of interest to examine the effect on metal–epoxide binding upon changing the substituents on the phenoxide ligands of cadmium from *tert*-butyl to phenyl, for we have previously noted that solutions of complex **2** in noncoordinating or weakly coordinating solvents are less receptive to adding neutral bases than are those of complex **1**.<sup>4e,14,23</sup> This trend in

(22) Roach, E. T.; Hardy, P. R.; Popov, A. I. *Inorg. Nucl. Chem. Lett.* **1973**, *9*, 359.

(23) (a) Darensbourg, D. J.; Zimmer, M. S.; Rainey, P.; Larkins, D. L. *Inorg. Chem.* **1998**, *37*, 2852. (b) Darensbourg, D. J.; Zimmer, M. S.; Rainey, P.; Larkins, D. L. *Inorg. Chem.* **2000**, *39*, 1578.

**Table 4.** Calculated Thermodynamic Parameters for the Reaction Defined in Eq 1<sup>a</sup>

epoxide	$\Delta H^\circ$ (kJ/mol)	$\Delta S^\circ$ (J/(K mol))	$\Delta G^\circ$ (kJ/mol)	$K_{\text{eq}}(298\text{K})$
cyclohexene oxide (2 equiv)	$-37.2 \pm 1.5$	$-123.2 \pm 6.4$	$-0.50 \pm 0.37$	1.23
cyclohexene oxide (4 equiv)	$-37.8 \pm 2.1$	$-125.1 \pm 8.9$	$-0.47 \pm 0.52$	1.21
<i>exo</i> -2,3-epoxynorbornane oxide (4.4 equiv)	$-33.9 \pm 0.8$	$-112.0 \pm 3.4$	$-0.49 \pm 0.19$	1.22

<sup>a</sup> Measurements carried out in methylene chloride.

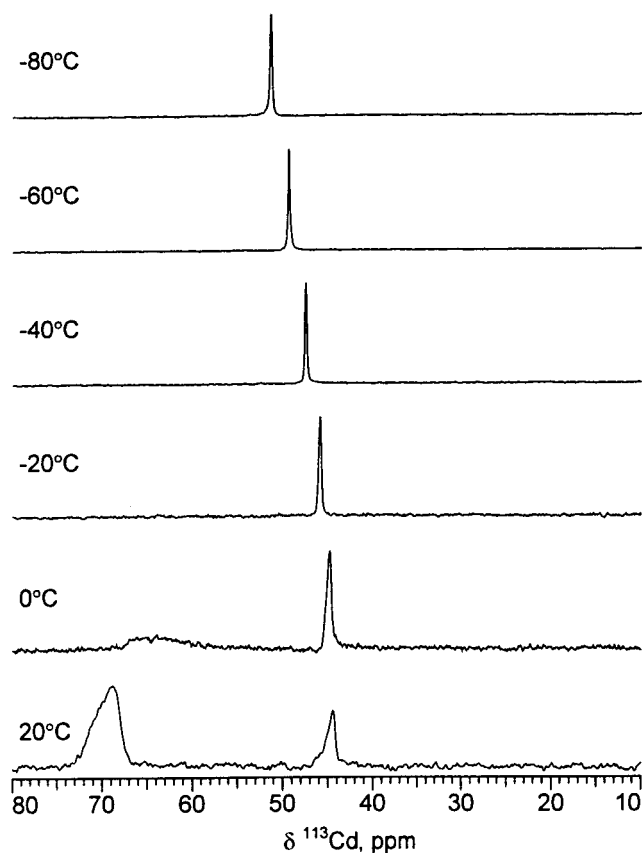


**Figure 11.** Temperature-dependent  $^{113}\text{Cd}$  NMR spectra of complex **2** in the presence of 20 equiv of cyclohexene oxide.

metal–ligand binding was thought to reflect greater steric requirements for the 2,6-diphenyl ligands. Figures 11 and 12 depict the  $^{113}\text{Cd}$  NMR spectra of two identically performed experiments involving the addition of 20 equiv of cyclohexene oxide and propylene oxide (PO), respectively, to complex **2** in *d*<sub>2</sub>-methylene chloride. As seen for other Lewis bases, complex **2** is less reactive toward epoxides when compared with complex **1**. For example, complex **1** undergoes almost complete formation of **monomer 1**·(CHO) in the presence of 4 equiv of epoxide at ambient temperature. By way of contrast, complex **2** in the presence of 20 equiv of CHO or PO at ambient temperature exists in rapid exchange with the **monomer 2**·(epoxide) mostly in the form of the dimer (recall that the  $^{113}\text{Cd}$  resonance for the dimer is found at 77.4 ppm). There is a slight preference of complex **2** reacting with CHO as compared to PO. Upon further lowering of the temperature the equilibrium defined in eq 1 for **monomer 2** is established with  $K_{\text{eq}}$  values of 1.27 and 0.547 at  $-40^\circ\text{C}$  for CHO and PO, respectively. From the temperature-dependent equilibrium constants,  $\Delta H^\circ$  values of  $-27.6$  and  $-29.9$  kJ/mol were determined. Hence, there is not a great deal of difference in the enthalpy values for reaction 1 as the phenoxide ligands are varied from 2,6-di-*tert*-butyl phenolate (see Table 4) to 2,6-diphenylphenolate. It is therefore possible

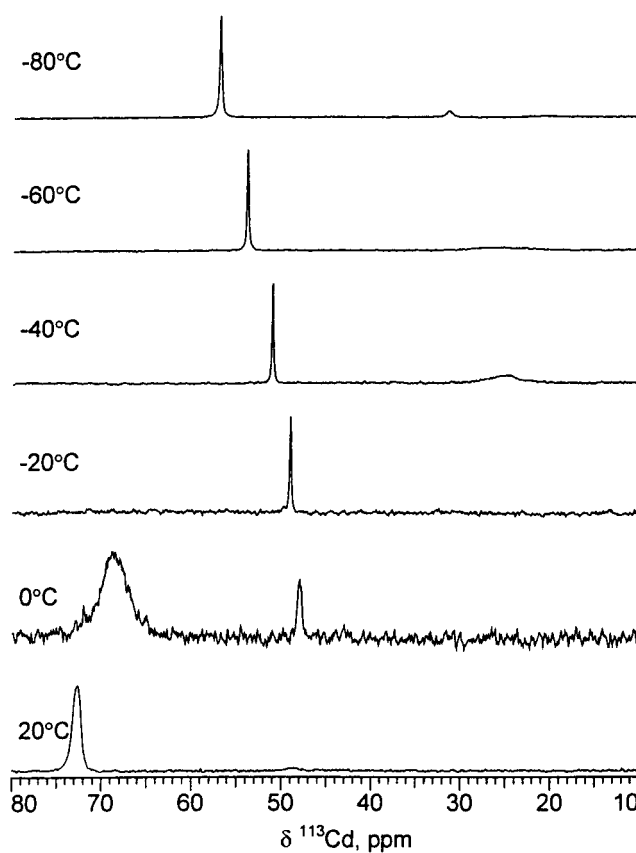
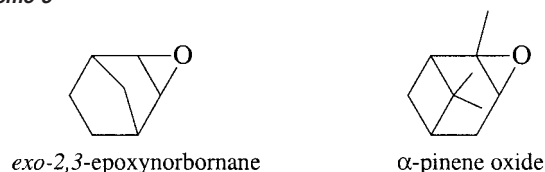


**Figure 12.** Temperature-dependent  $^{113}\text{Cd}$  NMR spectra of complex **2** in the presence of 20 equiv of propylene oxide.

to conclude from these studies that the reduction in reactivity of the dimeric complex **2** with Lewis bases as compared to complex **1** is the result of dimer **2** being inherently more stable. This added stability of complex **2** in solution is most likely due to additional metal interactions with the phenolate ligands via their aromatic substituents as is observed in the solid-state structure of **2** (vide supra).

As mentioned earlier, we are intensely interested in synthesizing 1:1 alternating copolymers of carbon dioxide and alicyclic epoxides other than cyclohexene oxide. This is in an effort to prepare polycarbonates with  $T_g$  values closer to that of bisphenol-A polycarbonate. That is, the  $T_g$  of poly(cyclohexane carbonate) at  $115^\circ\text{C}$  is some  $35^\circ\text{C}$  lower than that of bisphenol-A polycarbonate at  $150^\circ\text{C}$ , which dramatically limits the high-temperature applications of the former polycarbonate.<sup>6</sup> Therefore, it was desirable to employ bulkier, readily available epoxides such as  $\alpha$ -pinene oxide or *exo*-2,3-epoxynorbornane epoxides (Scheme 3) in hopes of preparing polycarbonate with higher  $T_g$  values than  $115^\circ\text{C}$ . It was felt that these bulky epoxides should show a decrease in internal motion of the polymer chains upon applying thermal energy. As a result, the restriction of intermolecular motion should raise the  $T_g$  values of the copolymer with respect to that of the cyclohexene oxide

Scheme 3



derived copolymer. Indeed, the pinene oxide derived copolymer might be semicrystalline.

Unfortunately, reactions of  $\alpha$ -pinene oxide or *exo*-2,3-epoxynorbornane under 65 bar of carbon dioxide pressure in the presence of  $[\text{Zn}(\text{O}-2,6\text{-}t\text{-Bu}_2\text{C}_6\text{H}_3)_2 \cdot \text{THF}]_2$  at 80 and 120 °C resulted in *no* copolymer production or other products resulting from  $\text{CO}_2$ /epoxide coupling reactions, such as cyclic carbonates. Under similar or milder reaction conditions, zinc bisphenoxide derivatives have proven to be extremely effective catalysts for the copolymerization of cyclohexene oxide and carbon dioxide to polycarbonates. Furthermore, mixtures of 70 mol % cyclohexene oxide and 30 mol %  $\alpha$ -pinene oxide or *exo*-2,3-epoxynorbornane were equally unsuccessful at producing terpolymers with carbon dioxide under these conditions. In these instances only poly(cyclohexene carbonate) was produced in greatly reduced yields due to competitive binding at the zinc center of the unreactive epoxides,  $\alpha$ -pinene oxide and *exo*-2,3-epoxynorbornane. Consistent with these negative observations, the zinc analogue of complex 1,  $[\text{Zn}(\text{O}-2,6\text{-}t\text{-Bu}_2\text{C}_6\text{H}_3)_2]$ , rapidly catalyzes the homopolymerization of cyclohexene oxide to polyethers at ambient temperature, making it extremely difficult to obtain single crystals of  $\text{Zn}(\text{O}-2,6\text{-}t\text{-Bu}_2\text{C}_6\text{H}_3)_2 \cdot (\text{CHO})_2$ . However, it is unreactive at homopolymerizing *exo*-2,3-epoxynorbornane, instead affording stable crystals of  $\text{Zn}(\text{O}-2,6\text{-}t\text{-Bu}_2\text{C}_6\text{H}_3)_2(\text{exo-2,3-epoxynorbornane})_2$  (**7**). The X-ray structure of complex **7** was found to be isostructural to that observed for its cadmium analogue, complex **5**. Indeed, the metal oxygen bond distance differences of 0.18 and 0.20 Å are very close to the difference in covalent radii of zinc and cadmium (0.17 Å). A thermal ellipsoid representation of complex **7** is shown in Figure 13, with comparative selected bond distances and bond angles to those of its cadmium analogue being listed in Table 5. Hence, it is obvious that the lack of activity displayed by zinc bisphenoxide derivatives for the homopolymerization of  $\alpha$ -pinene oxide or *exo*-2,3-epoxynorbornane to polyethers or the copolymerization of these epoxides and carbon dioxide to polycarbonates is not the result of the epoxides not binding to the metal center, but instead due to a higher reaction barrier for the epoxide ring-opening process.

## Summary

This study has demonstrated that phenoxides containing sterically demanding substituents (*t*-Bu or Ph) in the 2,6-positions can nevertheless serve as ligands capable of forming bisphenoxide derivatives of cadmium which exist as dimers both in the solid state and in weakly coordinating solvents. These dimeric complexes are readily disrupted in methylene chloride solution by a variety of epoxides leading to crystalline bisepoxide adducts of  $[\text{Cd}(\text{O}-2,6\text{-}R_2\text{C}_6\text{H}_3)_2]$ . Indeed, these complexes represent some of the few metal derivatives containing bound epoxides as ligands which have been characterized by X-ray crystallography. In methylene chloride solution  $^{113}\text{Cd}$  NMR spectroscopy has shown the reaction between the cadmium

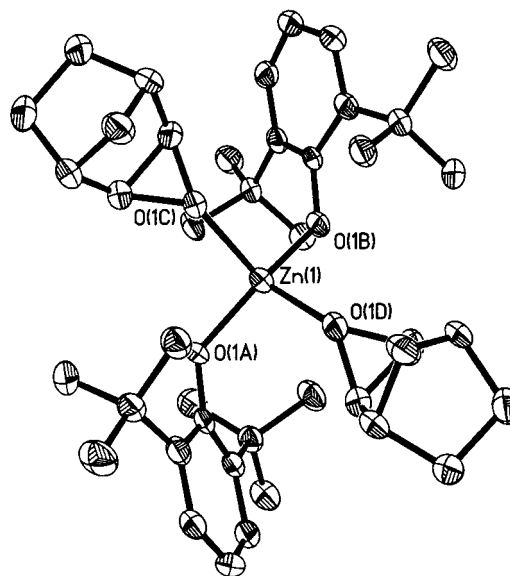


**Figure 13.** Thermal ellipsoid representation of complex **7**,  $[\text{Zn}(\text{O}-2,6\text{-}t\text{-Bu}_2\text{C}_6\text{H}_3)_2](\text{exo-2,3-epoxynorbornane})_2$ .

**Table 5.** Comparative Selected Bond Distances (Å) and Bond Angles (deg) in  $\text{M}(\text{O}-2,6\text{-}t\text{-Bu}_2\text{C}_6\text{H}_3)_2 \cdot (\text{exo-2,3-epoxynorbornane})_2$  Complexes

	Zn	Cd
av M–O <sub>(phenoxide)</sub>	1.880[3]	2.063[5]
av M–O <sub>(epoxide)</sub>	2.108[3]	2.307[5]
O <sub>ep</sub> –M–O <sub>ep</sub>	112.69(12)	114.37(19)
O <sub>phen</sub> –M–O <sub>phen</sub>	143.64(13)	147.6(2)
av O <sub>ep</sub> –M–O <sub>phen</sub>	99.95[12]	98.65[19]
av C–O–M	134.4[2]	130.85[5]

<sup>a</sup> Average standard derivatives in bond angles and distances are given in brackets.

dimers and epoxides to be sequential, with initial formation of the *mono* adduct at ambient temperature followed by a rapid equilibrium process leading to bisadduct formation as the temperature is lowered. From the  $^{113}\text{Cd}$  NMR spectra, equilibrium constants as a function of temperature for epoxide binding were determined which revealed little difference in binding between  $[\text{Cd}(\text{O}-2,6\text{-}t\text{-Bu}_2\text{C}_6\text{H}_3)_2]$  and cyclohexene oxide or *exo*-2,3-epoxynorbornane, as well as the other epoxides such as propylene oxide and  $\alpha$ -pinene. Although the relative affinity for epoxide binding of these epoxides to the  $[\text{Cd}(\text{O}-2,6\text{-}t\text{-Bu}_2\text{C}_6\text{H}_3)_2]$  derivative was comparable, there was a slight diminution in the binding to cadmium. The similarity of the binding abilities of the epoxides, cyclohexene oxide and *exo*-2,3-epoxynorbornane, to group 13 metal centers is in stark contrast to the reactivity of these systems for affecting epoxide ring-opening reactions. For example, whereas  $[\text{Zn}(\text{O}-2,6\text{-}t\text{-Bu}_2\text{C}_6\text{H}_3)_2]$  rapidly catalyzes cyclohexene oxide homopolymerization to polyether or copolymerization with carbon dioxide to polycarbonate, it only reacts with *exo*-2,3-epoxynorbornane to afford the stable, crystallographically characterized  $\text{Zn}(\text{O}-2,6\text{-}t\text{-Bu}_2\text{C}_6\text{H}_3)_2 \cdot (\text{exo-2,3-epoxynorbornane})_2$  complex. In part this difference in behavior of cyclohexene oxide and *exo*-2,3-epoxynorbornane is due to the reduction in epoxide ring strain energy for the latter epoxide, which we estimate to be about 8 kcal/mol.

Finally, a few words are warranted with regard to the unanticipated geometry noted herein and elsewhere for  $\text{Cd}(\text{O}-2,6\text{-}t\text{-Bu}_2\text{C}_6\text{H}_3)_2\text{L}_2$  (L = neutral donor ligand) derivatives.<sup>9,16</sup> That



is, in all instances with the exception of the one case reported upon here ( $L = \textit{exo}$ -2,3-epoxynorbornane) the cadmium center displays square-planar geometry in the presence of weakly coordinating ligands such as THF, THT, propylene carbonate, and epoxides. On the other hand, when  $L$  is a strongly donating ligand such as  $\text{PMe}_3$ , the expected distorted tetrahedral geometry is observed.<sup>24</sup> Previously, Buhro and co-workers have addressed this issue in a qualitative manner for the first observed THF adduct in terms of a linear bisphenoxide cadmium model with two weakly ligating neutral bases.<sup>21</sup> The distorted tetrahedral structure determined for complex **5** would not be accommodated by this explanation alone. Presently, we are carrying out rigorous computational studies on the zinc and cadmium complexes, and our preliminary results indicate that although there is a

(24) Darensbourg, D. J.; Rainey, P.; Larkins, D. L.; Reibenspies, J. H. *Inorg. Chem.* **2000**, *39*, 473.

significant difference in energy for the tetrahedral and square-planar geometries in  $\text{Zn}(\text{O}-2,6\text{-}^i\text{Bu}_2\text{C}_6\text{H}_3)_2\text{L}_2$  derivatives, the cadmium analogues show only a small difference in the stability of the two geometries. Nevertheless, the tetrahedral form is favored in both instances. These computational investigations will be reported in detail upon their completion.

**Acknowledgment.** Financial support from the National Science Foundation (CHE 99-10342 and CHE 98-07975 for the purchase of X-ray equipment) and the Robert A. Welch Foundation is greatly appreciated.

**Supporting Information Available:** Complete experimental details of the X-ray diffraction studies on complexes **1–5** and **7** (PDF). This material is available free of charge via the Internet at <http://pubs.acs.org>.

JA020184C